Comprehensive assessment and scenario simulation for the future of the hydrological processes in Dez river basin, Iran

Mohammad Reza Eini, Saman Javadi, Mehdy Hashemy Shahdany and Ozgur Kisi

ABSTRACT

Climate change is one of the leading factors that directly affect hydrological processes in large basins. This study assesses the impacts of climate change on streamflow, sediment and crop yield, actual evapotranspiration (AET), and water budget. In addition, the effects of land use and land cover (LULC) alteration with climate change on streamflow and sediment yield have been evaluated in the Dez river basin in the southwest of Iran. Five General Circulation Models (GCMs) based on two scenarios, Representative Concentration Pathway (RCP) 4.5 and RCP 8.5 for the near period (2021–2040) are considered. Hydrological simulation is performed using the Soil and Water assessment tool (SWAT) with good performance in the calibration (1990 to 2010) and validation (2010 to 2017) periods. The precipitation and temperature projected show a major upward trend related to the base period. The results showed that climate change increases the runoff and sediments. In addition, results projected that garden crop yields would increase while agricultural crop yields would decrease. In addition, AET will face a slight decline of about 2%–6%. Combined LULC and climate change scenarios showed that with amplification of orchards areas, sediment load would decrease.

Key words | crop simulation, Dez dam, land use change, sediment, Zagros Mountains

Mohammad Reza Eini
Saman Javadi (corresponding author)
Mehdy Hashemy Shahdany
Department of Irrigation and Drainage Engineering,
College of Aburaihan,
University of Tehran,
Tehran,
Iran
E-mail: *javadis@ut.ac.ir*

Ozgur Kisi
Faculty of Natural Sciences and Engineering,
Ilia State University,
0162 Tbilisi,
Georgia

HIGHLIGHTS

- Climate change increases the runoff and sediments.
- Evaluate the impacts of climate change on streamflow, sediment yield, crop yield, actual evapotranspiration, and water budget.
- Set up a comprehensive model for multifunctional calibration of hydrological processes.

INTRODUCTION

Universal climate change is one of the leading factors that directly affect hydrological processes (Zhang *et al.* 2016). In this regard, global warming is recognized as a significant issue for climate change during the coming century (Chien *et al.* 2013). Possible impacts of changes in climate including temperature and rainfall have caused variations in hydrological processes such as evapotranspiration, surface runoff, timing, and magnitude of streamflow, and flood events (Neupane & Kumar 2015). Since these impacts are expected to have diverse influences across a region, different spatial and temporal distributions are created for water resources components. Furthermore, the studies show that variation in precipitation patterns plays a vital role in streamflow trends and sediment in various regions across the United

doi: 10.2166/ws.2020.363

States (Novotny & Stefan 2007). Moreover, temperature variation and wind speed affect evaporation and transpiration sub-processes, which directly have an influence on the surface and subsurface water budgets (Schmid *et al.* 2000; Hu *et al.* 2007; Bajracharya *et al.* 2018).

It worth mentioning that researchers have indicated that climate change has an observable effect on long-term hydrologic processes, while in the short-term, Land Use and Land Cover (LULC) is one of the leading factors that have influence on catchment hydrologic processes (López-Moreno *et al.* 2013; Ficklin *et al.* 2016). LULC changes due to climate change, have influence on hydrological processes by conversion in hydrological components (Memarian *et al.* 2014; Deng *et al.* 2018). LULC changes cause variation in vegetation cover and surface roughness alteration and this affects the timing and magnitude of surface runoff and infiltration. The latter has led to changes in streamflow and consequently has influenced the magnitude and frequency of floods (Schilling *et al.* 2014). However, land use changes, such as urbanization and agricultural extension, may cause greater surface runoff (Pai & Saraswat 2011). Urban areas generate significant paved areas in the landscape, considered as impervious surfaces that produce greater surface that runoff as only small amounts of precipitation can soak into the soil profile. Intensive agricultural activities have led to a greater runoff because of reducing surface roughness and contributed to lower interception and less pore space availability in the soil (Busman & Sands 2002; Ghaffari *et al.* 2010; Baker & Miller 2013).

Accurate hydrological simulation of a basin needs developed models to consider a wide range of detailed information including the list of cultivated crops and orchards, irrigation schedules, fertilization and harvesting operations and so on (Eini 2019). This detailed information, which constitutes the inputs for distributed simulation models like Soil and Water Assessment Tool (SWAT), significantly describes percolation and evapotranspiration. A common belief is that without an accurate and complete calibration and validation of a model for local conditions of the system, no additional useful analyses in respect of the model estimates are reliable (Smarzyńska & Miatkowski 2016).

Researchers have shown that the effects of climate change on various agricultural products will not have a predictable trend due to the type of product, conditions of the case study, and climate scenarios (Shahvari *et al.* 2019). In some studies, increased crop yields have been reported and, in others, a drop in crop yields has been reported (Boonwichai *et al.* 2019; Kolberg *et al.* 2019). The result of a study in 10 largest producing countries showed that compared to present conditions, a group of 11 crop models found a rise in yield loss risk of 12%, 6.3%, 19.4% and 16.1% for wheat, corn, rice and soybeans by 2100, respectively (Leng & Hall 2019). Earlier studies have assessed the potential impact of water shortages under different climate situations on crop production in the USA, China, Australia, South Africa, and on a global scale (Shi & Tao 2014; Araújo *et al.* 2016; Madadgar *et al.* 2017; Matiu *et al.* 2017; Pirttioja *et al.* 2019).

This objective is fulfilled by employing semi distributed and fully distributed hydrological models, capable of simulation of the entire hydrological process under different climate and LULC changes. In this regard, the SWAT has been widely used to investigate agricultural practices, crop yields, and land management impacts on water quantity and quality considering climate change scenarios (Arnold & Fohrer 2005). Considering the capabilities of the SWAT model, different aspects of LULC alteration and climate change on sedimentation, soil erosion, and runoff magnitude have been investigated. Ngo *et al.* (2015) evaluated runoff and sediment in the Northwest of Vietnam using SWAT. The results showed that LULC status has a major influence on runoff and sediment yield. Land use conversion by extension of forested area and employment of soil protection practices over five years (2005 to 2010), had led to a decrease in both runoff (from 342.7 to 167.6 mm) and sediment yield (from 148.1 to 74.0 ton/ha).

To estimate climate conditions in the future, the Atmosphere-Ocean General Circulation Models (AOGCMs) and Regional Climate Models (RCMs) considering various CO_2 emission scenarios have been usually employed (Vaighan *et al.* 2017). An AOGCM is a type of climate model. It employs a mathematical model of the general circulation of a planetary atmosphere or ocean. It uses the Navier–Stokes equations on a rotating sphere with thermodynamic terms for various energy sources (radiation, latent heat). These equations are the basis for computer programs used to simulate the Earth's atmosphere or oceans. Atmospheric and Oceanic GCMs (AGCM and OGCM) are key components, along with sea ice and land-surface components.

GCMs and global climate models are used for weather forecasting, understanding the climate, and forecasting climate change. However, to assess the hydrological impacts of climate change, statistical or dynamic downscaling is essential. To achieve this objective, pre-defined statistical relationships or dynamical downscaling utilizing an RCM nested in a AOGCM is mostly employed (Marengo *et al.* 2009). Only a few studies have focused on the Representative Concentration Pathways (RCP) scenarios dependent on the Fifth Assessment Report (AR5), while many studies have used old AOGCMs under SRES (AR4) scenarios (Vaighan *et al.* 2017; Fernández *et al.* 2018). Chattopadhyay *et al.* (2017) investigated the potential climate change impacts on hydrologic processes in the Kentucky river basin, USA utilizing SWAT and CMIP5 GCMs considering RCP 4.5 and 8.5. According to their results, simulated surface runoff and monthly water yield indicated upward trends in the autumn and spring, while winter months were faced with downward trends. In similar studies, the possible effect of climate change was predicted to be more evident in the Himalayan region, where the runoff is dominated, primarily, by glacier melt and snowmelt (Bajracharya *et al.* 2018).

The aim of the current study was to evaluate the impacts of climate change on streamflow, sediment yield, crop yield, actual evapotranspiration, and water budget and the effect of LULC alteration on streamflow and sediment yield in the Dez river basin in the southwest of Iran. The novelty of this study is to set up a comprehensive model for multi-functional calibration of hydrological processes. Similar to other water-limited regions of the Middle East, food and water security are the main concerns in Iran (Ashraf *et al.* 2018). The study area is very susceptible to climate change impacts because of its high dependency on climate-sensitive agriculture (Ashraf *et al.* 2018). Moreover, the basin plays an undeniable role in the economic sector, where supplying agricultural water and energy production are the main concerns. According to the mentioned studies, although these scenarios have been employed in a few studies of basins throughout the world, reasonable outcomes have been reported. The results of this study will provide reliable guidelines, ensuring sustained water accessibility by changing climate and land use, for policymakers and water resources authorities within the study area.

CASE STUDY

The basin of the Dez river is a sub-basin of the Karoon Basin and is located in a more significant division in the Persian Gulf basin (Figure 1). Total surface area of the Dez watershed is approximately 17,320 km^2 and its perimeter is roughly 875 km. Major cities in this basin are Aligoudarz, Azna, and Broujerd. This basin is situated in the highlands of the western and southeastern Zagros Mountains and it is considered as the most densely populated area of the country, the dominant atmospheric precipitation in this region is snowy in the autumn and winter seasons (October to March). A large portion of annual runoff from the basin originates from melting snows from late winter to late spring (March to May). Sezar and Bakhtiari are the main branches of the Dez river.

Table 3 shows the land use area (ha) and percent in Dez river basin. Texture of the soil ranges between loam, sandy loam, sandy clay loam and loamy coarse sand. The topographical elevation varies between 728 m to 2,543 m with an average elevation of roughly 1,300 m, and average slope of 51% (Noori *et al.* 2016). According to the discharge stations, about 50% of the Dez river discharge at the Talezang station is related to the Bakhtiari subbasin and 42% of it is from the Sezar subbasin. The long-term trend of hydrological 185 events along with 290 flood events in the Dez river basin has been evaluated for a 50-year period (1955–2005). Results indicate that the peak flows of 17 flood events (52% of the total floods) were over 2,900 m^3/s from 1991 to 2005, while these values were normal from 1955 to 1990 (Samadi *et al.* 2019). Average precipitation in the study area is 700 mm with maximum and minimum temperatures of 27 °C and 12 °C, respectively. We used weather data (precipitation (mm), maximum and minimum temperature (°C)) and discharge data (Sezar, Bakhtiari, Dam, and Talezang discharge stations) for the calibration (1990 to 2010) and validation (2010 to 2017) periods.

MATERIALS AND METHODS

The analyses were conducted in five steps (Figure 2), steps: (1) Developing SWAT model; (2) uncertainty analysis calibration and validation of the SWAT hydrologic model for

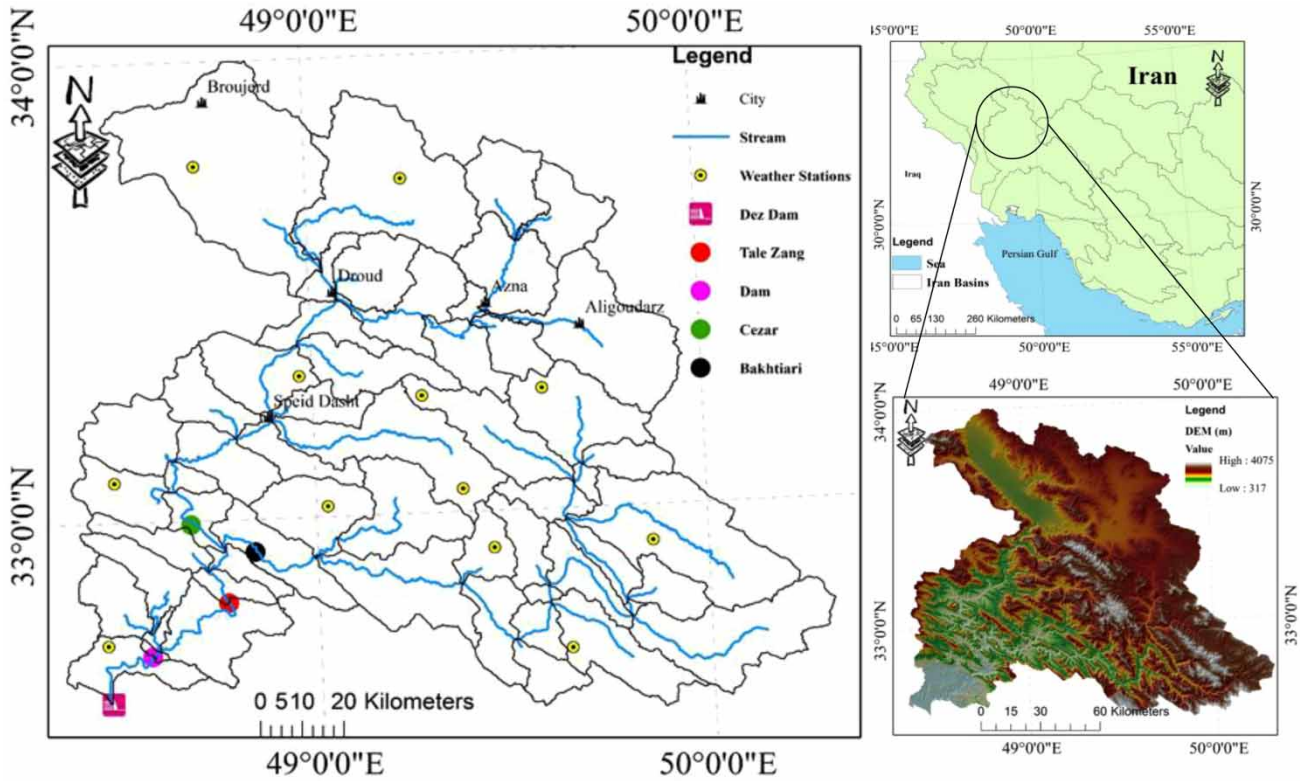

Figure 1 | Location of the study area, stream networks, cities, Dez dam, positions of discharge and weather stations and digital elevation map (DEM) in the Dez river basin.

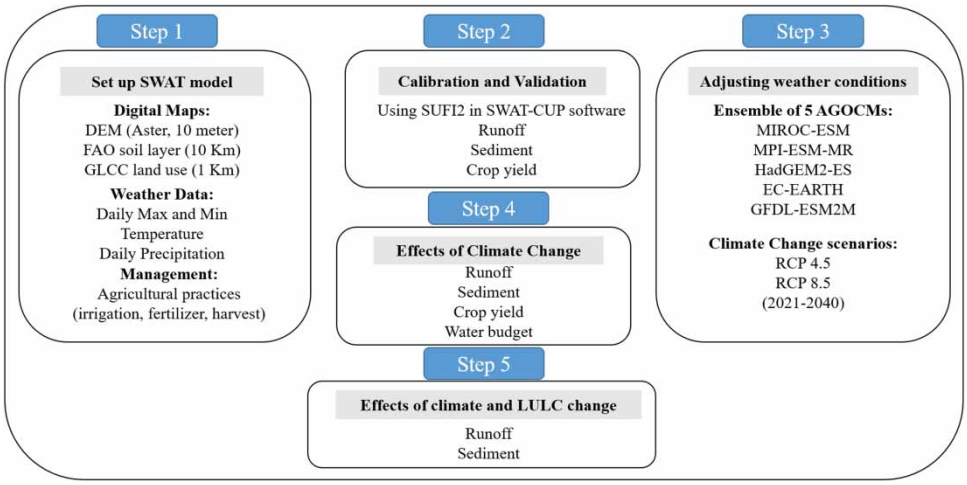

Figure 2 | Schematic representation of the methodology.

the test case of the study; (3) Developing climate change model via employing five AOGCM models considering two RCP scenarios (RCP 4.5 and RCP 8.5); (4) Assessing climate change effects on hydrological process; and (5) Assessing effects of climate change and LULC on runoff and sediment.

Developing the SWAT model

The SWAT is a long-term, continuous, physically distributed model developed for predicting the effect of land management practices on the hydrology, sediment yield, and water quality in agricultural watersheds (Arnold *et al.* 2012b; Jeon *et al.* 2019). The model can be operated in various time scales from a sub-daily time step to monthly/yearly duration one (Eini *et al.* 2019). According to Neitsch *et al.* (2011), computational simulation costs can be minimized within the Hydrologic Respond Unit (HRU) delineating process by combining similar soil and land-use areas into a single unit (Eini *et al.* 2020).

Hydrologic output and pollutant losses are initially generated at the HRU level, which are then aggregated to the sub-basin level and routed to the catchment outlet. The US Department of Agriculture (USDA) Natural Resources Conservation Service (NRCS) runoff curve number (CN) method is used to simulate the partitioning of precipitation at the soil surface between runoff and infiltration for daily time step simulations (USDA-NRCS 2004; Arnold *et al.* 2012a; Williams *et al.* 2012). The Green and Ampt Mein Larson (GAML) excess rainfall method (Mein & Larson 1973) is also available to partition precipitation between surface runoff and infiltration for sub-daily time step applications (Jeong *et al.* 2010; Arnold *et al.* 2012a; Brighenti *et al.* 2019).

The SWAT model can be utilized for sediment yield predictions for planning and management of water resources and reservoir sediment controls at the catchment scale (Op de Hipt *et al.* 2019). The fundamental factor controlling sediment yield, in general, is the transport capacity of runoff. Sediment transport in the channel network is a function of degradation and aggradation (Neitsch *et al.* 2011). The version of the SWAT model employed here routes the maximum sediment amount in a reach as a function of the peak channel velocity and calculates sediment yield for each HRU utilizing Modified Universal Soil Loss Equation (MUSLE). The sediment yield transported to the surface runoff was computed using the MUSLE (Bonumá *et al.* 2014). For individual HRU, the MUSLE equation of sediment yield $\mathrm{SED}_{j,k}$ (t/ha/year) is provided by the Equation (1):

$$\mathrm{SED}_{j,k} = 11.8\,(Q_{j,k}q_{j,k}A_{j,k})^{0.56}K_{j,k}C_{j,k}P_{j,k}LS_{j,k}\mathrm{CFRG}_{j,k} \quad (1)$$

In Equation (1), $Q_{j,k}$ denotes the volume of surface runoff related with the HRU (m^3), $q_{j,k}$ is the peak runoff rate (m^3/s), $K_{j,k}$ is the soil erodibility factor, $C_{j,k}$ is the crop management factor, $P_{j,k}$ is the conservation practice factor, $LS_{j,k}$ is the topographic factor, and $\mathrm{CFRG}_{j,k}$ is the coarse fragment factor. The complete description of the MUSLE is well recognized and utilized worldwide for investigation of water erosion (Djebou 2018).

In this study, ArcSWAT2012 is used as a visual interface to prepare a SWAT model (version 2012) within ESRI ArcMap 10.2. To set up the model, a 10 m digital elevation map, the global soil map produced by the FAO (Fischer *et al.* 2008) with a resolution of 10 km and the GLCC (https://lta.cr.usgs.gov/glcc/globe_int) land use map with resolution of 1 km are provided. Potential evapotranspiration calculation was carried out using the Hargreaves method that only needs daily minimum and maximum temperatures as input.

According to Figure 1, the watershed test case was divided into 57 sub-basins, 318 HRUs, and the managerial data, including amount of irrigation water for cultivated crops in the current cropping pattern (involving spring wheat, winter wheat, tomato, almond, and apple) and fertilizers of agricultural units, were incorporated into the model.

In addition, observed daily maximum and minimum temperatures were used from the existing 12 meteorological stations within the watershed. The time applied to evaluate the accuracy of the climate datasets was assigned for 1990–2017. For hydrologic modeling, the time period of 1990–1992 was determined as the warm-up period, while the periods of 1993–2010, and 2010–2017 were chosen for the calibration and the validation, respectively.

Management data

The type of agricultural products, the amount of irrigation according to location changes of agricultural products in the basin, irrigation efficiency, amount of urea fertilizer, plant growth period, and the range of yield changes in different areas of the basin are presented in Table 1. According to the available information, irrigation took place at 10-day intervals based on the plant's water requirement; fertilization was performed during the first irrigation. Furthermore, changes in the observed performance of

Table 1 | The cultivated crops management data in Dez river basin including irrigation water supplied water resource, efficiency, fertilizers, growth period, and crop yields

	Irrigation					
Crop	**Amount (mm)**	**Source**	**Efficiency**	**Fertilizer (kg/ha)**	**Growth period**	**Crop yield (ton/ha)**
Winter wheat	Rainfed	Precipitation	–	100	Dec–July	2.3–5.1
Spring wheat	370–410	Reach	0.37	250	Apr–Sep	2.3–6.5
Tomato	700–830	Reach	0.37	350	May–Sep	15.9–31.8
Almond	750–1,000	Reach	0.37	350	Apr–Sep	8–26.1
Apple	700–1,000	Reach	0.37	350	Apr–Oct	8.5–27.5

agricultural products in this drainage basin are indicated in Figure 6. According to Table 1, the average yield of winter wheat is 3.2, almond 19, spring wheat 4.7, apple 20.7 and tomato 22 tons per hectare.

Also according to the information provided by the Iranian Meteorological Organization (IMO) and CROPWAT: A Computer Program for Irrigation Planning and Management (www.fao.org/land-water/databases-and-software/cropwat/en/) the actual evapotranspiration of each agricultural product has been studied in the modeling process. The yields of agricultural products and actual evapotranspiration are moderate and estimated to be in the basin. Hence, it is not possible to simulate agricultural yield and actual evapotranspiration as a time series and they were evaluated on an average basis (Epelde *et al.* 2015). Observed actual evapotranspiration changes in the box plot concerning different points in the basin are indicated in Figure 6. The actual average evapotranspiration of winter wheat is 463 mm, almond is 902 mm, spring wheat is 614 mm, and apple is 891 mm and tomato 765 mm.

Agricultural products are calibrated based on the average basin drainage data including actual evapotranspiration and an average yield of agricultural products in SWAT-CUP software. In the calibration of agricultural yield, one of the most important parameters is the amount and type of fertilizer used for plants. Likewise, the soil parameters such as depth of root development (RDMX) and soil depth (SOL_Z) are primary parameters that should be investigated initially and simultaneously with runoff simulation. Sol_BD and Sol_AWC parameters, which are respectively related to soil porosity and water holding capacity of the soil, not only are critical in runoff simulation but also play a significant role in the calibration of plant yield. The values of these parameters highly influence the plants' water reception and water stress. Conversely, BLAI, T_BASE, T_OPT, and BIO_E are important parameters for agricultural products that are separately described in Table 10.

The yields of agricultural products in the SWAT model are based on the dry weight of agricultural products; in other words, the amount of water in agricultural products in the outputs of the SWAT model is reduced, and the dry weight of yield is shown as the output in the model (Neitsch *et al.* 2011). However, when the agricultural products are harvested, they are wet and, to solve this problem, the amount of water in each product should be added to the outputs of the model. Therefore, according to the data available at the USDA database (https:/ndb.nal.usda.gov/ndb/foods), the amount of water found in each product was obtained and added to the outputs of the model. These changes were made as follows. Also, Table 2 shows the percentage of water available in each agricultural product. In Equation (2), the calculation of the crop yield (ton/ha) of agricultural products is shown. Table 3 shows the land use area (ha) and percent in the Dez river basin:

$$\text{Real Crop yield} = \text{Crop yield (simulation)} + \text{Crop yield (simulation)} \times \text{Water content} \quad (2)$$

Calibration and uncertainty analysis of the outcomes produced by the model were implemented utilizing the SUFI2 algorithm in the SWAT-CUP software (Abbaspour *et al.* 2015). This technique permits setting ranges for the parameters of interest and afterward running multiple simulations with various parameter sets sampled by Latin hypercube. In this study, Nash–Sutcliffe Efficiency (NSE) objective function was assigned, and the software returned

Table 2 | Water content within the crops

Crop	Water content (%)		Source
	Minimum	Maximum	
Winter wheat	0.1	0.15	https:/ndb.nal.usda.gov/ndb/foods
Spring wheat	0.1	0.15	
Tomato	0.85	0.95	
Almond	0.03	0.07	
Apple	0.75	0.85	

Table 3 | Area (ha) and land use percent of the study area

Land Use	Area (ha)	Percent
Almonds	70,450.41	4.19
Apple	70,450.41	4.19
Grassland	984,866.8	58.6
Shrubland	445,219.4	26.49
Spring Wheat	38,517.52	2.29
Tomato	21,516.12	1.28
Winter Wheat	35,049.34	2.09
Residential-Medium Density	1,266.142	0.08
Savanna	4,027.387	0.24
Sparsely vegetated	398.7911	0.02
Water bodies	9,017.945	0.54

the range of predicted uncertainty within the 95% of the best simulations. Furthermore, to compare the performance of models, the statistical indices of NSE (Equation (3)) and R^2 (Equation (4)) were used. Table 4 demonstrates the equations utilized to compute every statistical metric, where: N is the number of samples; O_i is observed value (surface runoff (m^3/s)) for day i; M_i is the model output (surface runoff (m^3/s)) for day i; and M_{avg}, O_{avg} represent average of model output and observed data (Duan *et al.* 2016).

Downscaling of AOGCMs

In this research, five AOGCM considering two RCP scenarios, RCP 4.5 and RCP 8.5, were applied for the near period (2021–2040). Appendix A shows the selected climate model for this study. These scenarios were obtained from WDC Climate website (https://cera-www.dkrz.de/WDCC/ui/cerasearch). Table 5 shows changes in precipitation, and also maximum and minimum temperatures. For coupling of five AOGCMs, an average of monthly changes was used.

The resolution of the GCMs is too wide for a local appraisement; hence, downscaling was performed using SWAT. The change factor downscaling method was performed to change the observed daily average temperature and precipitation utilizing Equations (5) and (6), respectively. The change factor process is regularly utilized to eliminate or diminish the bias among observations and the GCMs outputs (Bekele *et al.* 2018). The change factor process relies on the adjustment of the daily time step series of the climate variables, by including the monthly average changes of GCMs (Bekele *et al.* 2018), where T_{adj} (P_{adj}) is the adjusted daily temperature (precipitation) for the future; T_{obs} (P_{obs}) is the observed daily temperature (°C) or precipitation (mm) for the historical years; $\bar{T}_{GCM,fut,\,i}$ ($\bar{P}_{GCM,fut,\,i}$) is the temperature (°C) or precipitation (mm) for the historical of the AOGCM outputs for the future years; $\bar{T}_{GCM,base,\,i}$ ($\bar{P}_{GCM,base,\,i}$) is the monthly mean temperature (precipitation) of the AOGCM outputs for the base period; w_i is the weight of each grid cell; and k is the

Table 4 | Statistical indices for estimating the accuracy of the simulation

Index	Unit	Equation	Range of index	Equation
NSE	–	$\mathrm{NSE} = 1 - \left[\frac{\sum_1^N (O_i - M_i)^2}{\sum_1^N (O_i - O_{avg})^2}\right]$	$-\infty$ – 1	3
R^2	–	$R^2 = \left[\frac{\sum_1^N (O_i - O_{avg})(M_i - M_{avg})}{\sqrt{\sum_1^N (O_i - O_{avg})^2}\sqrt{(M_i - M_{avg})^2}}\right]^2$	0–1	4

Table 5 | Average changes of precipitation and temperature under RCP4.5 and RCP8.5 scenarios

	Rain (mm)		Temp-min (°C)		Temp-max (°C)	
Month	**RCP 4.5**	**RCP 8.5**	**RCP 4.5**	**RCP 8.5**	**RCP 4.5**	**RCP 8.5**
Jan	0.96	1	0.8	1.3	1.1	1.66
Feb	0.8	0.95	0.75	1.37	1.28	1.77
Mar	0.79	0.98	0.95	1.44	1.51	1.72
Apr	0.91	1.02	1.1	1.47	1.65	1.7
May	1.02	1.07	1.27	1.53	1.84	1.78
Jun	1.01	1.1	1.66	1.92	2.24	3.14
Jul	0.87	1.18	1.8	2.23	2.51	3.44
Aug	0.76	1.15	1.9	2.22	2.48	3.43
Sep	0.79	0.95	1.87	2.15	2.31	2.32
Oct	0.83	0.98	1.65	2	2.05	2.12
Nov	0.86	1.1	1.25	1.68	1.75	1.81
Dec	0.98	1.08	1.07	1.36	1.34	1.58

number of the grid cells:

$$T_{adj} = T_{obs} + \frac{\sum_{j=1}^{k} (\bar{T}_{GCM,fut,\,i} - \bar{T}_{GCM,base,\,i})}{k} \quad (5)$$

$$P_{adj} = P_{obs} + \frac{\sum_{j=1}^{k} (\bar{P}_{GCM,fut,\,i}/\bar{P}_{GCM,base,\,i})}{k} \quad (6)$$

The percentage of precipitation changes under each of the scenarios and the maximum and minimum increase in temperature of each of the scenarios are presented in Figure 3. The highest drop in rainfall is predicted in the RCP4.5 scenario (24% decrease) in August, and the highest increase is expected to be in July under the RCP8.5 scenario. Furthermore, in scenario RCP8.5, the maximum temperature shows an increase of 3 °C in the summer months (June-August). Table 5 is the combination of (ensemble) variations of the five selected models which display precipitation values relative to the base period and the absolute changes in temperature.

Water budget and land use land cover changes

Hydrological assessments within a watershed scale need a reliable water budget for management and evaluation of the future. Based on this concept, water budget components were calculated in the form of a historical period and future. Precipitation, snowmelt, actual and potential evapotranspiration, shallow aquifer recharge, and deep aquifer recharge were then calculated.

The average long-term rainfall in this watershed is about 683 mm, which is known as the input of the hydrological cycle. Other components of the hydrological cycle are infiltration 87 mm (13%), runoff 184 mm (27%) and AET 412 mm (60%) (Table 6).

To study and evaluate the effects of the LULC extreme change, three land use change scenarios were assigned for the developed model. The scenarios are: (i) change of crops (spring wheat, tomato, and winter wheat) to orchards

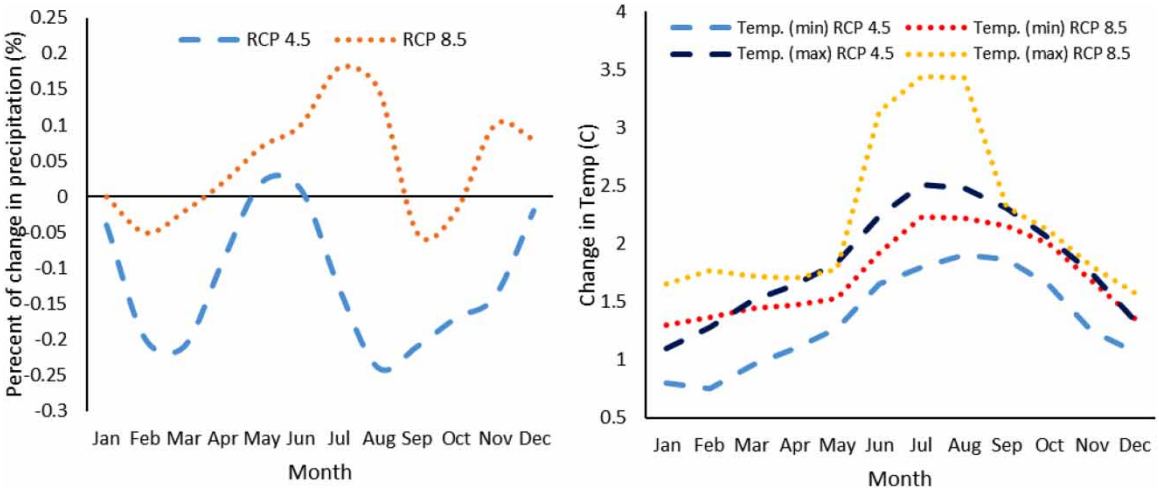

Figure 3 | Maximum and minimum temperature and precipitation fluctuations under the climate change scenarios.

Table 6 | Water budget components of the Dez river basin (based on the gathered information in this study)

Components (mm)	Base period (based on Iran's Ministry of Energy report)
Precipitation	683
Runoff	184
Infiltration	87
AET	412

(almond and apple), (ii) green pasture (grassland) to bare lands (shrub land), and (iii) spring wheat to winter wheat (rainfed). Also, changes in runoff and sediment were calculated for each scenario for the near future (2021–2040) and under all RCPs.

RESULTS AND DISCUSSION

Runoff and sediment simulation

To ascertain that the calibrated models are representative of the hydrological response in the watershed simulated monthly runoff and sediment in discharge stations were carried out. Moreover, crop yield and AET of five major agricultural products were calibrated. According to Figure 1, four discharge stations are located in the basin. For runoff calibration and validation, the entire stations were included and for sediment just one station, an outlet of the watershed, was included due to lack of appropriate data. First, by selecting various parameters in SWAT-CUP and performing the model by 500 iterations applying the SUFI2 algorithm, sensitive parameters have been selected by *P*-value and *t*-Stat (Table 7). To complete both the runoff and sediment simulation, NSE and R^2 indices were selected as goodness of fit factors. In most of the hydrological simulations, NSE and R^2 should be more than 0.6 to have acceptable results for prediction of future and management practices (Arnold *et al.* 2012b; Anand *et al.* 2018).

In this research, the SWAT model showed reasonable performance in runoff and sediment calibration and validation in the entire discharge stations. Table 7 shows calibrated parameters values and their sensitive ranking. The lowest *P*-value with the highest absolute value of *t*-Stat indicates the most sensitive parameter and vice versa. According to the results, CN2.mgt, TLAPS.sub, and GW_REVAP.gw were recognized as the most sensitive parameters for runoff simulation in this watershed. Also, in Figure 4 time series of calibration and validation have been shown. Table 8 shows NSE and R^2 values in calibration (1990–2010) and validation (2010–2017) periods.

As mentioned earlier, the parameters given in Table 7 were used in the simulation of sediment. The results of statistical indices indicated that the developed SWAT model for the study area has a high accuracy in both calibration and validation phases. In accordance with the obtained results in Figure 5 and Table 9, both of the simulated time series and the statistical indices achieved the high accuracy of the developed model.

In a study by Arnold *et al.* (2012b), the most sensitive and widely used parameters of the SWAT model presented are similar to the parameters selected in this study. In addition, in the Nilawar & Waikar (2019) study in India, calibration parameters selected for runoff and sediment are similar to the selected parameters of the present study which have achieved excellent results (NSE and R2 ~ 0.91 to 0.62) in runoff and sediment simulation. Also, in another research conducted by Anand *et al.* (2018) in India with a SWAT model, good results, i.e. NSE and R^2 were more than 0.75, were obtained in 26 discharge stations. Finally, the similarity of results of this study and its selected parameters with the mentioned articles and other studies such as Ayivi & Jha (2018), conducted in North Carolina, and Visakh *et al.* (2019), conducted in India, reflects the high precision of the SWAT model developed in this study in the simulation of runoff and sediment and prediction of the future. It can be seen that in all of the mentioned studies, the SWAT model is accepted as a powerful model in hydrological simulation.

Model performance in crop yield and AET

According to the variation interval of each plant parameter of the SWAT model, the yield of agricultural products was calibrated. Subsequently, the average yield of each agricultural product in all HRUs was calculated and compared with the observed values. Similarly, considering that AET is a function of the growth and yield of agricultural products, this balance component was also examined and compared

Table 7 | Main parameters used for sensitivity and calibration in SWAT

Rank	Parameter name	*t*-Stat	*P*-value	Fitted value	Min	Max	Description
Runoff sensitive parameters, final range and fitted values							
1	R__CN2.mgt	−27.24	0	−0.313	−0.35	0.35	SCS runoff curve number
2	V__TLAPS.sub	5.36	0	−3.950	−5	5	Temperature lapse rate
3	V__GW_REVAP.gw	−4.47	0	0.119	0.02	0.2	Groundwater revap. coefficient
4	V__PLAPS.sub	4.05	0	178.200	−300	300	Precipitation lapse rate
5	V__GWQMN.gw	−3.98	0	19.950	10	2,000	Threshold depth of water in shallow aquifer for return flow to occur
6	R__HRU_SLP.hru	2.44	0.02	0.232	−0.55	0.55	Average slope steepness
7	R__SOL_BD(2).sol	1.82	0.07	0.003	−0.55	0.55	Moist bulk density of first soil layer
8	R__SOL_AWC(2).sol	−1.46	0.15	−0.078	−0.55	0.55	Soil available water storage capacity
9	R__SURLAG.bsn	1.34	0.18	−0.090	−0.35	0.35	Surface runoff lag time
10	V__GW_DELAY.gw	−1.13	0.26	44.415	30	45	Groundwater delay time
11	R__SOL_BD(1).sol	0.79	0.43	0.465	−0.55	0.55	Moist bulk density of first soil layer
12	R__SLSUBBSN.hru	−0.77	0.44	0.190	−0.35	0.35	Average slope length
13	R__LAT_TTIME.hru	0.76	0.45	−0.085	−0.35	0.35	Lateral flow travel time
14	V__REVAPMN.gw	0.6	0.55	86.100	0	100	Threshold depth of water in the shallow aquifer for 'revap' to occur (mm)
15	V__ALPHA_BF.gw	−0.4	0.69	0.037	0	0.2	Base flow alpha factor
16	R__SOL_AWC(1).sol	−0.29	0.77	−0.140	−0.55	0.55	Soil available water storage capacity
Sediment sensitive parameters, final range and fitted values							
1	v__SPEXP.bsn	−7.5	0	0.978	0.84	1.27	Exponent parameter for calculating sediment re-entered in channel sediment routing
2	v__SPCON.bsn	6	0	0.0021	0	0.01	Linear parameter for calculating sediment re-entered in channel sediment routing
3	v__CH_COV1.rte	3.57	0	0.11	0	0.32	Channel erodibility factor
4	v__CH_COV2.rte	−1.5	0.14	0.887	0.48	1.43	Channel cover factor
5	v__USLE_P.mgt	0.79	0.23	0.95	0.48	1.42	USLE equation soil erodibility P factor
6	v__USLE_K(1).sol	−0.69	0.37	0.32	0.17	0.53	USLE equation soil erodibility K factor
7	v__SED_CON.hru	−0.6	0.57	4,110	1,785	5,158	Sediment concentration in runoff
8	v__SLSOIL.hru	−0.24	0.69	44.47	0	98.8	Slope length for lateral subsurface flow
9	v__LAT_SED.hru	−0.16	0.73	1,169	0	3,114	Sediment concentration in lateral and groundwater flow

*R means relative change and V means replace.

to the observed data like the yield of agricultural products. Finally, based on location variations in products yield and AET, the NSE and R2 indexes were calculated. The values of plant parameters and their descriptions are separately presented in Table 10. Furthermore, the mean observed values and the results of the SWAT model for agricultural yield and AET are presented in Table 11.

In Table 11, average variations in yield of agricultural products and evapotranspiration show that simulated values are greater than observed values. This difference can be attributed to the fact that simulations have been carried out for a long period of time, and the average yield of the products has changed over time as a result of variations in temperature and precipitation, but observed data are available only for a few numbers of years. As observed from the correlation and error statistical indices in Table 11, these simulated values are reliable and the model has shown a good performance.

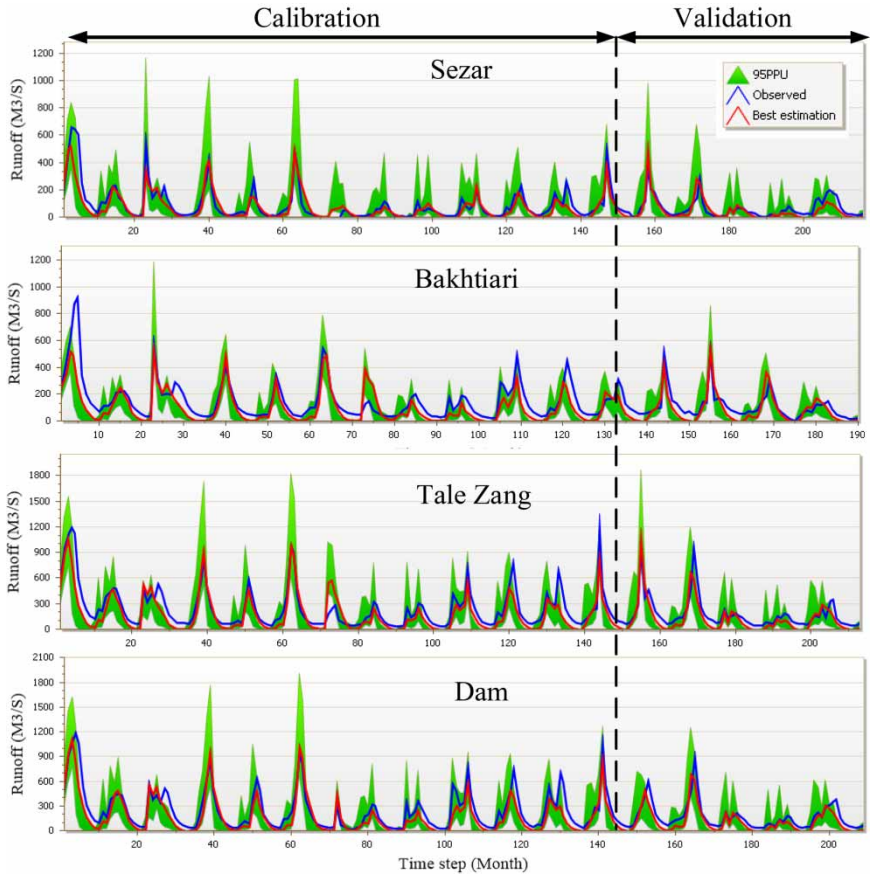

Figure 4 | Comparison of the simulated monthly runoff hydrograph with the observed data in calibration and validation periods with a 95% uncertainty.

Table 8 | Simulation results in calibration (1990–2010) and validation (2010–2017) periods

	Calibration		Validation	
Discharge station	**R^2**	**NSE**	**R^2**	**NSE**
Sezar	0.77	0.75	0.62	0.61
Bakhtiari	0.71	0.62	0.6	0.55
Tale Zang	0.81	0.74	0.61	0.69
Dam	0.84	0.77	0.7	0.7

In Figure 6, variations in the yield values of plant products as well as AET are shown in the observation period in the box-plot and the results of the SWAT model are indicated using black circle. The results of AET simulation and crop yield indicated that the SWAT model has a high ability to simulate plant. The results of the simulation of plant yield in spring wheat and winter wheat were very close to the observed values and the evapotranspiration of each of these products was higher than the average observed value. The two horticultural products used in the simulation have been estimated to be higher than 2.5 tons per hectare. Also, R^2 and NSE indices for apple, almond and wheat showed that these products had the best accuracy in simulation.

Comparing the results obtained in this study indicated that, in other studies, the SWAT model has a good accuracy in the estimation of agricultural yields. The results of Epelde *et al.* (2015), which simulated four major products (wheat, barley, potato, beet) in Spain, pointed out that the yield of agricultural products in the SWAT model is not well correlated annually, and it is necessary to use the average yield of agricultural products for evaluation of the simulation. In reality, due to changes in the behavior of farmers' communities by time, the advancement of agricultural technology, pests, government policies in water and agriculture sectors, the final cost and the benefits of agriculture have a direct impact on agricultural performance, but the SWAT model

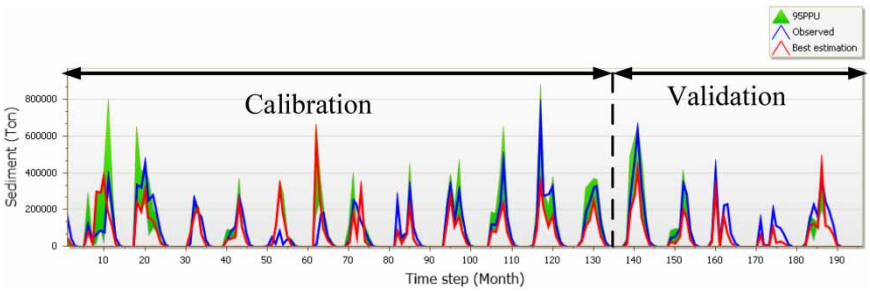

Figure 5 | The simulated and observed sediment time-series with the 95% uncertainty band for the Dez dam's inflow station.

Table 9 | Calculated values of the statistical indices in calibration and validation stages of sediment simulation

	Calibration				Validation			
Discharge station	**p-factor**	**r-factor**	**R^2**	**NS**	**p-factor**	**r-factor**	**R^2**	**NS**
Dam	0.73	0.53	0.66	0.62	0.33	0.57	0.61	0.59

Table 10 | Effective parameters on agricultural yield for crops in the cropping pattern

Parameter	**Winter wheat**	**Spring wheat**	**Tomato**	**Almond**	**Apple**	**Description**
BLAI	6	6.5	8	7.5	8	Max leaf area index
HVSTI	1	1	1	1	1	Harvest index
T_BASE	3	5	6	9	9	Min temp plant growth
T_OPT	17	23	25	20	23	Optimal temp for plant growth
EXT_COEF	3	3	3.8	3.4	3.4	Light extinction coefficient
BIO_E	75	75	85	75	75	Biomass/Energy Ratio
GSI	5	5	5	5	5	Max stomatal conductance
RDMX	1	1	1.5	3	3	Max root depth

Table 11 | Performance of SWAT model in crop yield and AET simulation

	Crop yield (ton/ha)		AET (mm)			
Crop	**Observed**	**Simulated**	**Observed**	**Simulated**	**R^2**	**NSE**
Winter wheat	3.2	3.6	463	499	0.65	0.69
Spring wheat	4.7	5.1	614	634	0.55	0.6
Tomato	22	24.5	765	770	0.57	0.55
Almond	19	21.5	902	925	0.59	0.67
Apple	20.7	22.5	891	932	0.63	0.71

does not have the ability to simulate and understand many of these factors. In addition, the simulation of climate change effects on agricultural products with the SWAT model in a basin in China was investigated in a study conducted by Niu *et al.* (2017). In this study, the main products of the region such as corn, spring wheat, spring barley, and spring canola-polish were investigated. The simulated agricultural products showed high correlation

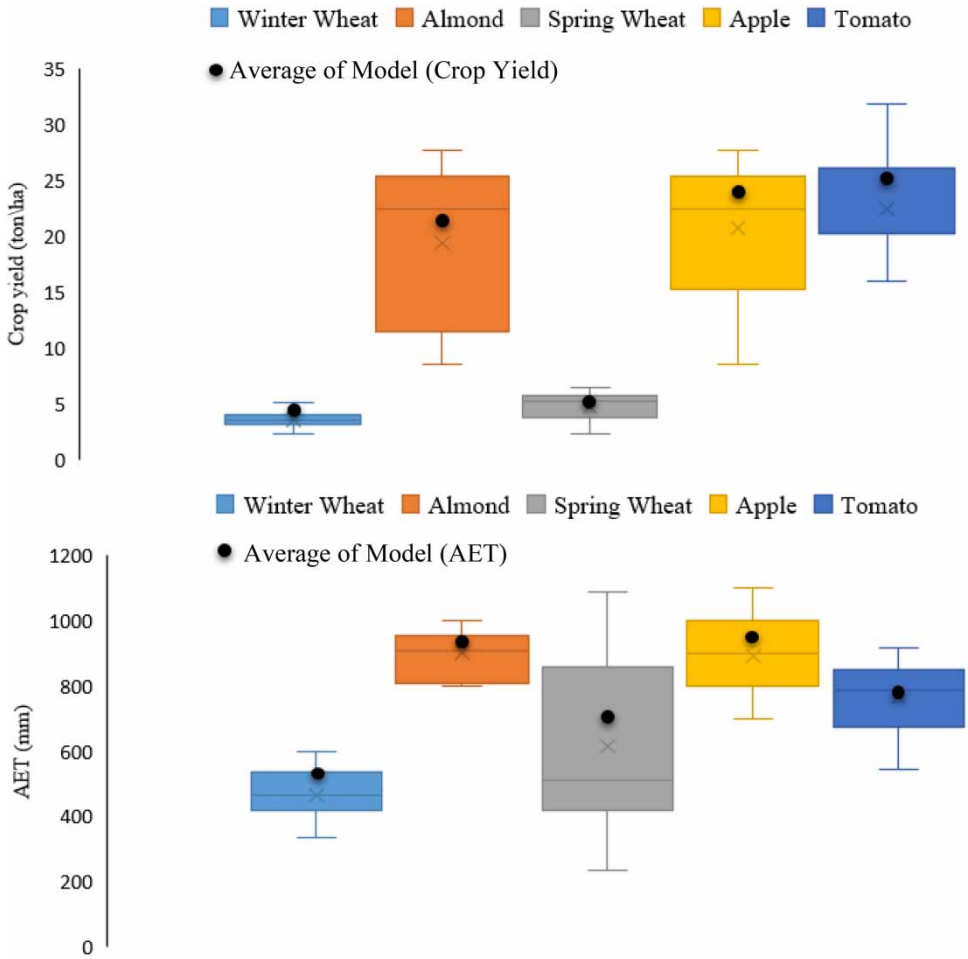

Figure 6 | Variation of crop yields and AET (box plots) in Dez river basin and average performance of model (point).

with the mean location observations using the coefficient R^2 (from 0.84 to 0.93). Similarly, the results of other studies such as Sinnathamby *et al.* (2017) and Daggupati *et al.* (2015) regarding the method of assessing the yield of agricultural products and the important parameters in the calibration of those products using the SWAT model approve the results of the present study.

Role of climate change on runoff and sediment

Monthly changes of precipitation and max–min temperatures were also applied to the developed SWAT model after calibration and validation. Runoff variations in RCP4.5 scenario did not show any unreasonable changes in the runoff amount, and changes will take place as time displacement. In addition, in the spring, there is an increase in runoff in all scenarios. For instance, in June 154 m^3/s in base period will change, for RCP 4.5 and RCP 8.5, to 205 m^3/s and 199 m^3/s respectively. Runoff variations in the RCP8.5 scenario indicated an increase in runoff magnitude during the spring and summer seasons. However, with an increase of about 3.5 degrees of melting temperature, this will happen earlier with more intense evapotranspiration.

As sediment load is soluble in the river, sediment load changes will change with runoff. However, it worth mentioning that either sediment producing sources or sediment active factors (including crop type, soil, and topography and so on) did not change with climate change.

By increasing runoff in winter times within the RCP4.5 and RCP 8.5 scenarios, sediment load will increase about 13%–19% in February. Likewise, in the spring and summer, the mentioned changes will have increasing

trends. For instance, sediment load will be increased under RCP scenarios around 30%–37%; 42%–49%; 54%–62%; respectively at July, August, and September. The latter occurred because of runoff increasing during these months. However, in the autumn, no reasonable significant changes will occur in sediment load, of course except the one in November by −12% decrease.

In general, it can be said that average runoff in the coming period will rise from 208 cubic meters per second in the baseline period to about 228 cubic meters per second in both scenarios (about 9% increase in each scenario). The results also showed that runoff variations in each scenario would be similar to each other, with a slight increase in the RCP8.5 scenario. Similar to these variations, sediment has also increased by 10% in each scenario. Figure 7 shows monthly changes in runoff and sediment.

The climate change effect on runoff and sediment variation by SWAT model in Purna river basin in India considering two scenarios of RCP4.5 and RCP8.5 showed

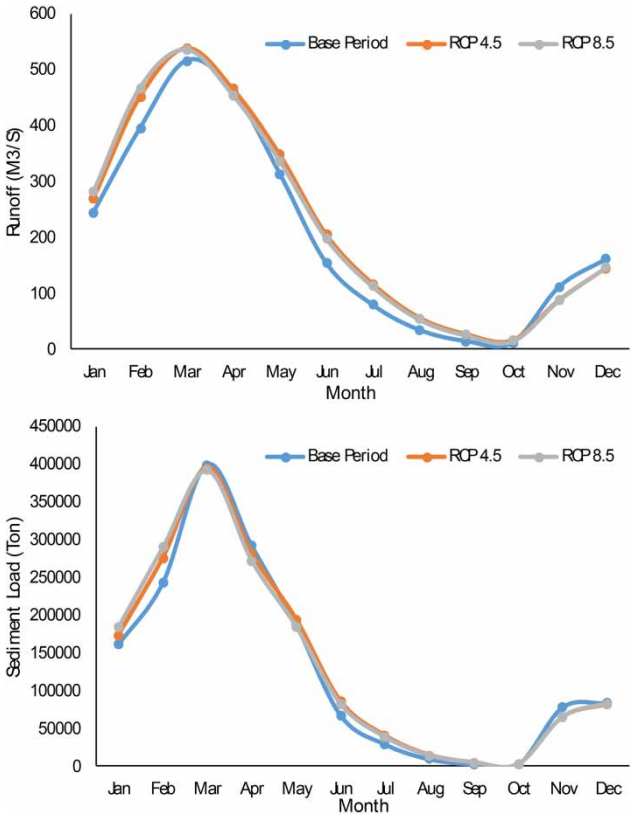

Figure 7 | Effect of climate change on runoff and sediment under RCP4.5 and RCP 8.5.

an increase from 7% to 17% for runoff and from 2% to 16% for sediment. These changes are similar to those of the present study (Nilawar & Waikar 2019). Moreover, Tan *et al.* (2017) estimated that surface runoff in all tropical regions of Malaysia would increase under all RCP scenarios in future periods between 14 and 27%. Conversely, in a basin in Alberta, Canada, it was found that sediment under the effect of climate change will face an increase of 5% to 25% in different regions (Shrestha & Wang 2018). Different results have been presented in other studies using the SWAT model and RCP scenarios. A study in Ethiopia has indicated that, under the influence of climate change and RCP 8.5 and RCP 4.5 scenarios, runoff will face a minor reduction (Serur & Sarma 2017). In China, Zhang *et al.* (2016) estimated that under RCP scenarios, significant changes will not occur in runoff in the upcoming periods.

Effect of climate change on crop yield and AET

Due to the effects of temperature increase and changes in precipitation pattern, the yield of agricultural products has reduced and the yield of horticultural products was slightly increased. The yield of almonds and apples in different locations increased on average about 3%–5% (1 ton per hectare) and 1%–7% (1.2 tons per hectare) in the scenario of RCP4.5 and 4%–9% (1.2 tons per hectare) and 5%–9% (1.4 tons per hectare) in the RCP8.5 scenario, respectively. Conversely, variations in winter wheat which was simulated as rain-fed wheat, showed a decreasing trend. As rain-fed wheat is planted in winter and harvested in the summer, temperature rise has had a negative effect on this product and a mean decrease of 7% to 25% (0.7 t/ha) was observed in different parts of the basin under RCP4.5 and RCP8.5 scenarios. Also, the variations in spring wheat yield (9%–19%) and tomato (4%–22%) declined and an average of 1 ton per hectare for spring wheat and 3.5 tons per hectare for tomato was estimated. Also, changes in evapotranspiration in the upcoming period indicated a decrease for all agricultural products (about 2% for horticultural products and about 6% for agricultural products) in different locations.

As irrigation and other operations of agricultural products have not changed, the long growth period of horticultural products and plant's remaining in soil

throughout the year have led to withstanding the increase in temperatures and subsequent increase in evapotranspiration. Due to displacement in terms of time and increased precipitation, horticultural plants have been able to supply their water needs and their growth course begins a little earlier than before.

In studies conducted on the change in yield of agricultural products influenced by climate change under the SRES scenarios in Iran, generally products yields have decreased in dry regions, while yields have increased in temperate, cold, and dry areas (Nazari 2015). In a study carried out by Parry *et al.* (2004) in Iran, yield of rain-fed products, especially wheat, is estimated to decrease about 5% to 40% by 2080. Also, in another study conducted by Nassiri *et al.* (2006), it was predicted that a decrease of about 18% to 24% will be observed in the wheat yield as the temperature rises from 2.7 to 4.7 °C. In 2015, it was estimated that in the central Zagros, in a part of which the basin is located, the yield of rain-fed products will decrease from 7% to 13%. Studies showed that peas, corn, and potatoes would have a yield reduction of 11% to 50% by 2100 (Lashkari *et al.* 2012; Moradi *et al.* 2013; Hajarpoor *et al.* 2014). According to the results of this study and comparison with other studies under SRES scenarios, we will face a declining trend in agricultural products in the future, while changes in horticultural products will relatively increase.

Effect of climate change on the water budget

After the hydrological simulation of the basin in the base and future periods, the water budget of the watershed was calculated. The parameters of precipitation, surface runoff, infiltration into the aquifer and AET have been calculated from the components of discharge in the catchment area. In the future, the changes will show a slight increase of about 5 mm in precipitation in both scenarios. In addition, the infiltration, which is a function of snow and snowmelt, will also be reduced from 11% to 9%. In each scenario, a surface runoff will be increased in the range of 26% to 29%. In addition, AET will increase relative to the base period (63% to 62%) but portion of AET will decrease relative to other water budget components (Table 12).

In an investigation conducted by Tan *et al.* (2017), in a basin in Malaysia it was estimated that under RCP scenarios, runoff components (14.6–27.2%) and AET (0.3–2.7%) would decrease. Also, in the Malaprabha basin in India, the combination of the five climatic models (GCMs) showed that AET increased by 4.1% and water demand for agriculture increased by 7.7%, while penetration would decrease by 7.3% (Reshmidevi *et al.* 2018). Also Nazari (2015) estimated that under the SRES scenarios, 10.3% of available water is expected to decrease in the same basin. Another study in the Weyib Basin in Kenya revealed that under RCP scenarios, runoff and evapotranspiration will decline (Serur & Sarma 2017). According to the performed studies, it can be concluded that the effects of climate change in different locations can be different; there will be no significant changes in the balance parameters in this basin.

Effect of climate change and LULC on runoff and sediment

Three management scenarios regarding LULC changes were applied to investigate the effect of climate change on runoff and sediment. It is worth mentioning that the LULC scenarios were defined according to land use distributions of the study area.

Considering the major crops used in the model, the first scenario assumed that spring wheat and tomato have changed into apple and almond trees. In the second scenario, it is assumed that green grasslands, which contain grassy plants in spring and summer and contain about 58 percent of the area, have become bare lands. In the third scenario, assumption is that spring wheat (irrigated crop) has been changed to winter wheat (rainfed farming).

According to Figure 8, under the first scenario, LULC change in the SWAT model shows a reduction in runoff in comparison with changes in the existing LULC of the watershed. These changes occurred due to increased irrigation

Table 12 | Water budget components in base period and under climate change scenarios

Component	Base period (observed data)	Base period (model)	RCP 4.5	RCP 8.5
Precipitation	683	698.39	704.54	705.46
Runoff	184	177.69	199.01	205.78
Infiltration	87	73.75	63.7	61.12
AET	412	420.7	423.89	434.4

from the river, because the water requirement for the orchard's trees is more than the other crops in the region. For instance, major changes (about 5%) happened in May to July in RCP 8.5. In addition, sediment variations in this scenario has already shown a decrease in most months of the year. Under RCP 8.5 and RCP 4.5, sediment load has decreased by around 14% in summer.

In RCP scenarios, runoff has increased, in a range of 13%–19% under the second scenario of LULC changes. The increase happened compared to the base period due to replacing the water-repellent and water-consuming areas (i.e. plants and shrubs) by bare lands. Furthermore, sediment variations in this scenario have been shown to rise in most months of the year so that, under RCP 8.5 and RCP 4.5, the sediment load has increased by around 13% in summer.

Considering the change of spring wheat to winter wheat (rainfed) under the third scenario of the study, area has not been changed significantly relative to the assigned climate scenarios. LULC changes on base period indicate that monthly runoff has been affected in most of the year. The latter occurred due to the irrigation reduction in this scenario, which led to increasing transpiration, evaporation, vegetation in winter and spring as well. Because the planting date for winter wheat is about four months earlier than spring wheat, during this time it decreases due to plant growth as well as changes in the surface cover of the runoff area. In addition, sediment in this scenario has been shown to rise in most months of the year. Under RCP 8.5 and RCP 4.5, sediment load has been increased by around 19% in summer.

In Figure 8, the runoff and sediment changes are shown relative to the base period. Moreover, all LULC scenarios that had been applied under climate change are given in appendices B and C.

In the study by Ngo *et al.* (2015), it was determined that, under the impact of increase in agricultural lands, the expansion of urban areas will increase runoff and sediment; in addition, increase in forest cover and implementation of soil conservation scenarios will reduce runoff and sediment.

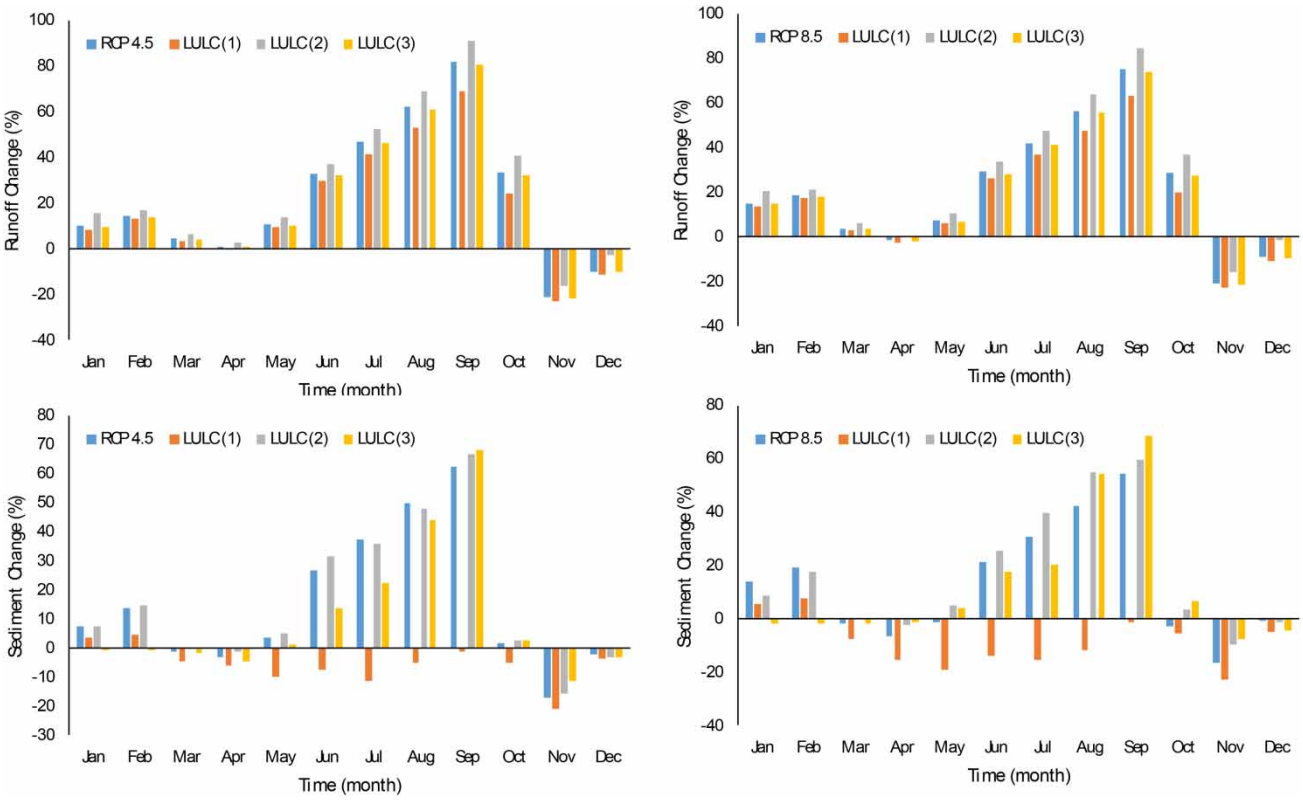

Figure 8 | Monthly changes in runoff and sediment under LULC and climate change relative to base period.

CONCLUSION

In his study, the SWAT model was utilized to simulate the Dez river dam basin in Iran. In general, the climate change scenarios (RCP4.5, RCP8.5) did not predict unfavorable situations in the future.

The model indicated a high capability to simulate the runoff and sediment, (average accuracy of 0.75). The results of the climate change scenarios showed that climate change increases the runoff values, for example, an increase from 154 m^3/s to 205 and 199 m^3/s was projected for runoff, and an increase from 13 to 19% was projected for sediments. Also, agricultural yield changes under the influence of two scenarios showed that horticultural crop yields would increase while agricultural crop yields would decrease. Furthermore, the AET will face a slight decline of 2% to 6%.

Results showed that, in the future, the watershed will face a slight increase in runoff and AET. Combined LULC and climate change scenarios showed that with amplification of orchards, sediment load would decrease.

In this research, multisite downscaling method in the SWAT model was applied. We would like to suggest that researchers use different multisite downscaling methods, like quantile mapping and bias correction. In addition, in the current research, it was not possible to add groundwater simulation. So, it is highly recommended to use SWAT-MODFLOW to simulate the interaction between groundwater and surface water.

DATA AVAILABILITY STATEMENT

All relevant data are included in the paper or its Supplementary Information.

REFERENCES

Abbaspour, K. C., Rouholahnejad, E., Vaghefi, S., Srinivasan, R., Yang, H. & Kløve, B. 2015 A continental-scale hydrology and water quality model for Europe: calibration and uncertainty of a high-resolution large-scale SWAT model. *Journal of Hydrology* **524**, 733–752.

Anand, J., Gosain, A. K., Khosa, R. & Srinivasan, R. 2018 Regional scale hydrologic modeling for prediction of water balance, analysis of trends in streamflow and variations in streamflow: the case study of the Ganga River basin. *Journal of Hydrology: Regional Studies* **16**, 32–53.

Araújo, M. B., Ferri-Yáñez, F., Bozinovic, F., Chown, S. L. & Marquet, P. A. 2016 Erratum to Araújo *et al.* (2013). *Ecology Letters* **19** (5), 591–592.

Arnold, J. G. & Fohrer, N. 2005 SWAT2000: current capabilities and research opportunities in applied watershed modelling. *Hydrological Processes: An International Journal* **19** (3), 563–572.

Arnold, J., Kiniry, J., Srinivasan, R., Williams, J., Haney, E. & Neitsch, S. 2012a *Soil and Water Assessment Tool, Input/Output File Documentation, Version 2012*. Texas Water Research Institute, Technical Report 439, College Station, Texas.

Arnold, J. G., Moriasi, D. N., Gassman, P. W., Abbaspour, K. C., White, M. J., Srinivasan, R., Santhi, C., Harmel, R., Van Griensven, A. & Van Liew, M. W. 2012b SWAT: Model use, calibration, and validation. *Transactions of the ASABE* **55** (4), 1491–1508.

Ashraf, S., AghaKouchak, A., Nazemi, A., Mirchi, A., Sadegh, M., Moftakhari, H. R., Hassanzadeh, E., Miao, C.-Y., Madani, K., Mousavi Baygi, M., Anjileli, H., Arab, D. R., Norouzi, H., Mazdiyasni, O., Azarderakhsh, M., Alborzi, A., Tourian, M. J., Mehran, A., Farahmand, A. & Mallakpour, I. 2018 Compounding effects of human activities and climatic changes on surface water availability in Iran. *Climatic Change* **152**, 379–391.

Ayivi, F. & Jha, M. K. 2018 Estimation of water balance and water yield in the reedy fork-buffalo creek watershed in North Carolina using SWAT. *International Soil and Water Conservation Research* **6**, 203–213.

Bajracharya, A. R., Bajracharya, S. R., Shrestha, A. B. & Maharjan, S. B. 2018 Climate change impact assessment on the hydrological regime of the Kaligandaki Basin, Nepal. *Science of The Total Environment* **625**, 837–848.

Baker, T. J. & Miller, S. N. 2013 Using the soil and water assessment tool (SWAT) to assess land use impact on water resources in an East African watershed. *Journal of Hydrology* **486**, 100–111.

Bekele, D., Alamirew, T., Kebede, A., Zeleke, G. & Melesse, A. M. 2018 Modeling climate change impact on the Hydrology of Keleta watershed in the Awash River basin, Ethiopia. *Environmental Modeling & Assessment* **24**, 1–13.

Bonumá, N. B., Rossi, C. G., Arnold, J. G., Reichert, J. M., Minella, J. P., Allen, P. M. & Volk, M. 2014 Simulating landscape sediment transport capacity by using a modified SWAT model. *Journal of Environmental Quality* **43** (1), 55–66.

Boonwichai, S., Shrestha, S., Babel, M. S., Weesakul, S. & Datta, A. 2019 Evaluation of climate change impacts and adaptation strategies on rainfed rice production in Songkhram River Basin, Thailand. *Science of The Total Environment* **652**, 189–201.

Brighenti, T. M., Bonumá, N. B., Srinivasan, R. & Chaffe, P. L. B. 2019 Simulating sub-daily hydrological process with

SWAT: a review. *Hydrological Sciences Journal* **64** (12), 1415–1423.

Busman, L. & Sands, G. 2002 *Agricultural Drainage: Issues and Answers*. University of Minnesota Extension Service, MI-07740.

Chattopadhyay, S., Edwards, D. & Yu, Y. 2017 Contemporary and future characteristics of precipitation indices in the Kentucky River Basin. *Water* **9** (2), 109.

Chien, H., Yeh, P. J.-F. & Knouft, J. H. 2013 Modeling the potential impacts of climate change on streamflow in agricultural watersheds of the Midwestern United States. *Journal of Hydrology* **491**, 73–88.

Daggupati, P., Pai, N., Ale, S., Douglas-Mankin K, R., Zeckoski R, W., Jeong, J., Parajuli P, B., Saraswat, D. & Youssef M, A. 2015 A recommended calibration and validation strategy for hydrologic and water quality models. *Transactions of the ASABE* **58** (6), 1705–1719.

Deng, C., Liu, P., Wang, D. & Wang, W. 2018 Temporal variation and scaling of parameters for a monthly hydrologic model. *Journal of Hydrology* **558**, 290–300.

Djebou, D. C. S. 2018 Assessment of sediment inflow to a reservoir using the SWAT model under undammed conditions: a case study for the Somerville reservoir, Texas, USA. *International Soil and Water Conservation Research* **6**, 222–229.

Duan, Z., Liu, J., Tuo, Y., Chiogna, G. & Disse, M. 2016 Evaluation of eight high spatial resolution gridded precipitation products in Adige Basin (Italy) at multiple temporal and spatial scales. *Science of The Total Environment* **573** (Supplement C), 1536–1553.

Eini, M. R. 2019 Discussion of 'Intra- and interannual streamflow variations of Wardha watershed under changing climate' (2018) by Naga Sowjanya P., Venkata Reddy K. & Shashi M. (ISH Journal of Hydraulic Engineering, DOI: 10.1080/09715010.2018.1473057). *ISH Journal of Hydraulic Engineering* 1–2. DOI:10.1080/09715010.2018.1564376

Eini, M. R., Javadi, S., Delavar, M., Monteiro, J. A. F. & Darand, M. 2019 High accuracy of precipitation reanalyses resulted in good river discharge simulations in a semi-arid basin. *Ecological Engineering* **131**, 107–119.

Eini, M. R., Javadi, S., Delavar, M., Gassman, P. W. & Jarihani, B. 2020 Development of alternative SWAT-based models for simulating water budget components and streamflow for a karstic-influenced watershed. *CATENA* **195**, 104801.

Epelde, A., Cerro, I., Sánchez-Pérez, J., Sauvage, S., Srinivasan, R. & Antigüedad, I. 2015 Application of the SWAT model to assess the impact of changes in agricultural management practices on water quality. *Hydrological Sciences Journal* **60** (5), 825–843.

Fernández, J., Frías, M. D., Cabos, W. D., Cofiño, A. S., Domínguez, M., Fita, L., Gaertner, M. A., García-Díez, M., Gutiérrez, J. M., Jiménez-Guerrero, P., Liguori, G., Montávez, J. P., Romera, R. & Sánchez, E. 2018 Consistency of climate change projections from multiple global and regional model intercomparison projects. *Climate Dynamics* **52** (1–2), 1139–1156.

Ficklin, D. L., Robeson, S. M. & Knouft, J. H. 2016 Impacts of recent climate change on trends in baseflow and stormflow in United States watersheds. *Geophysical Research Letters* **43** (10), 5079–5088.

Fischer, G., Nachtergaele, F., Prieler, S., van Velthuizen, H., Verelst, L. & Wiberg, D. 2008 *Global Agro-ecological Zones Assessment for Agriculture (GAEZ 2008)*. IIASA, Luxenburg, Austria and FAO, Rome, Italy.

Ghaffari, G., Keesstra, S., Ghodousi, J. & Ahmadi, H. 2010 SWAT-simulated hydrological impact of land-use change in the Zanjanrood basin, Northwest Iran. *Hydrological Processes: An International Journal* **24** (7), 892–903.

Hajarpoor, A., Soltani, A., Zeinali, E. & Sayyedi, F. 2014 Simulating climate change impacts on production of chickpea under water-limited conditions. *Agriculture Science Developments* **3** (6), 209–217.

Hu, Q., Feng, S., Guo, H., Chen, G. & Jiang, T. 2007 Interactions of the Yangtze river flow and hydrologic processes of the Poyang Lake, China. *Journal of Hydrology* **347** (1–2), 90–100.

Jeon, D. J., Ligaray, M., Kim, M., Kim, G., Lee, G., Pachepsky, Y. A., Cha, D.-H. & Cho, K. H. 2019 Evaluating the influence of climate change on the fate and transport of fecal coliform bacteria using the modified SWAT model. *Science of The Total Environment* **658**, 753–762.

Jeong, J., Kannan, N., Arnold, J., Glick, R., Gosselink, L. & Srinivasan, R. 2010 Development and integration of sub-hourly rainfall–runoff modeling capability within a watershed model. *Water Resources Management* **24** (15), 4505–4527.

Kolberg, D., Persson, T., Mangerud, K. & Riley, H. 2019 Impact of projected climate change on workability, attainable yield, profitability and farm mechanization in Norwegian spring cereals. *Soil and Tillage Research* **185**, 122–138.

Lashkari, A., Alizadeh, A., Rezaei, E. E. & Bannayan, M. 2012 Mitigation of climate change impacts on maize productivity in northeast of Iran: a simulation study. *Mitigation and Adaptation Strategies for Global Change* **17** (1), 1–16.

Leng, G. & Hall, J. 2019 Crop yield sensitivity of global major agricultural countries to droughts and the projected changes in the future. *Science of The Total Environment* **654**, 811–821.

López-Moreno, J., Pomeroy, J., Revuelto, J. & Vicente-Serrano, S. 2013 Response of snow processes to climate change: spatial variability in a small basin in the Spanish Pyrenees. *Hydrological Processes* **27** (18), 2637–2650.

Madadgar, S., AghaKouchak, A., Farahmand, A. & Davis, S. J. 2017 Probabilistic estimates of drought impacts on agricultural production. *Geophysical Research Letters* **44** (15), 7799–7807.

Marengo, J. A., Jones, R., Alves, L. M. & Valverde, M. C. 2009 Future change of temperature and precipitation extremes in South America as derived from the PRECIS regional climate modeling system. *International Journal of Climatology: A Journal of the Royal Meteorological Society* **29** (15), 2241–2255.

Matiu, M., Ankerst, D. P. & Menzel, A. 2017 Interactions between temperature and drought in global and regional crop yield variability during 1961–2014. *PLoS One* **12** (5), e0178339.

Mein, R. G. & Larson, C. L. 1973 Modeling infiltration during a steady rain. *Water Resources Research* **9** (2), 384–394.

Memarian, H., Balasundram, S. K., Abbaspour, K. C., Talib, J. B., Boon Sung, C. T. & Sood, A. M. 2014 SWAT-based hydrological modelling of tropical land-use scenarios. *Hydrological Sciences Journal* **59** (10), 1808–1829.

Moradi, R., Koocheki, A., Mahallati, M. N. & Mansoori, H. 2013 Adaptation strategies for maize cultivation under climate change in Iran: irrigation and planting date management. *Mitigation and Adaptation Strategies for Global Change* **18** (2), 265–284.

Nassiri, M., Koocheki, A., Kamali, G. & Shahandeh, H. 2006 Potential impact of climate change on rainfed wheat production in Iran: (Potentieller Einfluss des Klimawandels auf die Weizenproduktion unter Rainfed-Bedingungen im Iran). *Archives of Agronomy and Soil Science* **52** (1), 113–124.

Nazari, M. R. 2015 The Economic Impacts of Climate Change on Iranian Agricultural Sector. *Technical Workshop Of Investigating Climate Change Related Challenges and Implementing the United Nations Framework Convention on Climate Change in Iran*, Tehran, Iran (In Persian).

Neitsch, S. L., Arnold, J. G., Kiniry, J. R. & Williams, J. R. 2011 *Soil and Water Assessment Tool Theoretical Documentation Version 2009*. Texas Water Resources Institute.

Neupane, R. P. & Kumar, S. 2015 Estimating the effects of potential climate and land use changes on hydrologic processes of a large agriculture dominated watershed. *Journal of Hydrology* **529**, 418–429.

Ngo, T. S., Nguyen, D. B. & Rajendra, P. S. 2015 Effect of land use change on runoff and sediment yield in Da River Basin of Hoa Binh province, Northwest Vietnam. *Journal of Mountain Science* **12** (4), 1051–1064.

Nilawar, A. P. & Waikar, M. L. 2019 Impacts of climate change on streamflow and sediment concentration under RCP 4.5 and 8.5: a case study in Purna river basin, India. *Science of The Total Environment* **650**, 2685–2696.

Niu, J., Kang, S., Zhang, X. & Fu, J. 2017 Vulnerability analysis based on drought and vegetation dynamics. *Ecological Indicators* **105**, 329–336.

Noori, H., Siadatmousavi, S. M. & Mojaradi, B. 2016 Assessment of sediment yield using RS and GIS at two sub-basins of Dez Watershed, Iran. *International Soil and Water Conservation Research* **4** (3), 199–206.

Novotny, E. V. & Stefan, H. G. 2007 Stream flow in Minnesota: indicator of climate change. *Journal of Hydrology* **334** (3–4), 319–333.

Op de Hipt, F., Diekkrüger, B., Steup, G., Yira, Y., Hoffmann, T., Rode, M. & Näschen, K. 2019 Modeling the effect of land use and climate change on water resources and soil erosion in a tropical West African catch-ment (Dano, Burkina Faso) using SHETRAN. *Science of The Total Environment* **653**, 431–445.

Pai, N. & Saraswat, D. 2011 SWAT2009_LUC: a tool to activate the land use change module in SWAT 2009. *Transactions of the ASABE* **54** (5), 1649–1658.

Parry, M. L., Rosenzweig, C., Iglesias, A., Livermore, M. & Fischer, G. 2004 Effects of climate change on global food production under SRES emissions and socio-economic scenarios. *Global Environmental Change* **14** (1), 53–67.

Pirttioja, N., Palosuo, T., Fronzek, S., Räisänen, J., Rötter, R. P. & Carter, T. R. 2019 Using impact response surfaces to analyse the likelihood of impacts on crop yield under probabilistic climate change. *Agricultural and Forest Meteorology* **264**, 213–224.

Reshmidevi, T., Kumar, D. N., Mehrotra, R. & Sharma, A. 2018 Estimation of the climate change impact on a catchment water balance using an ensemble of GCMs. *Journal of Hydrology* **556**, 1192–1204.

Samadi, A., Sadrolashrafi, S. S. & Kholghi, M. K. 2019 Development and testing of a rainfall-runoff model for flood simulation in dry mountain catchments: a case study for the Dez River Basin. *Physics and Chemistry of the Earth, Parts A/B/C* **109**, 9–25.

Schilling, K. E., Gassman, P. W., Kling, C. L., Campbell, T., Jha, M. K., Wolter, C. F. & Arnold, J. G. 2014 The potential for agricultural land use change to reduce flood risk in a large watershed. *Hydrological Processes* **28** (8), 3314–3325.

Schmid, W., Mecklenburg, S. & Joss, J. 2000 Short-term risk forecasts of severe weather. *Physics and Chemistry of the Earth, Part B: Hydrology, Oceans and Atmosphere* **25** (10), 1335–1338.

Serur, A. B. & Sarma, A. K. 2017 Impact of spatial data availability on climate change prediction in the Weyib River Basin in Ethiopia. *Water Resources Management* **31** (6), 1809–1824.

Shahvari, N., Khalilian, S., Mosavi, S. H. & Mortazavi, S. A. 2019 Assessing climate change impacts on water resources and crop yield: a case study of Varamin plain basin, Iran. *Environmental Monitoring and Assessment* **191** (3), 134.

Shi, W. & Tao, F. 2014 Vulnerability of African maize yield to climate change and variability during 1961–2010. *Food Security* **6** (4), 471–481.

Shrestha, N. K. & Wang, J. 2018 Predicting sediment yield and transport dynamics of a cold climate region watershed in changing climate. *Science of The Total Environment* **625**, 1030–1045.

Sinnathamby, S., Douglas-Mankin, K. R. & Craige, C. 2017 Field-scale calibration of crop-yield parameters in the Soil and Water Assessment Tool (SWAT). *Agricultural Water Management* **180**, 61–69.

Smarzyńska, K. & Miatkowski, Z. 2016 Calibration and validation of SWAT model for estimating water balance and nitrogen losses in a small agricultural watershed in central Poland. *Journal of Water and Land Development* **29** (1), 31–47.

Tan, M. L., Ibrahim, A. L., Yusop, Z., Chua, V. P. & Chan, N. W. 2017 Climate change impacts under CMIP5 RCP scenarios on water resources of the Kelantan River Basin, Malaysia. *Atmospheric Research* **189**, 1–10.

USDA-NRCS 2004 *National Engineering Handbook Hydrology Part 630*. US Department of Agriculture, Natural Resources Conservation Service, Washington, D.C.

Vaighan, A. A., Talebbeydokhti, N. & Bavani, A. M. 2017 Assessing the impacts of climate and land use change on streamflow, water quality and suspended sediment in the Kor River Basin, Southwest of Iran. *Environmental Earth Sciences* **76** (15), 543.

Visakh, S., Raju, P., Kulkarni, S. S. & Diwakar, P. 2019 Inter-comparison of water balance components of river basins draining into selected delta districts of Eastern India. *Science of The Total Environment* **654**, 1258–1269.

Williams, J., Kannan, N., Wang, X., Santhi, C. & Arnold, J. 2012 Evolution of the SCS runoff curve number method and its application to continuous runoff simulation. *Journal of Hydrologic Engineering* **17** (11), 1221–1229.

Zhang, Y., You, Q., Chen, C. & Ge, J. 2016 Impacts of climate change on streamflows under RCP scenarios: a case study in Xin River Basin, China. *Atmospheric Research* **178–179**, 521–534.

First received 30 March 2020; accepted in revised form 1 December 2020. Available online 14 December 2020